



Synthesis and Characterization of Soft Magnetic Materials $\text{Ni}_x\text{Zn}_{1-x}\text{Fe}_2\text{O}_4$ ($x = 0,2 - 0,8$) Lombok Iron Sand with Co-precipitation Method

Nining S. Asri^{1*}, Awan Maghfirah², Nesyia Izzania Batubara³

¹Research Center for Physics, Indonesian Institute of Sciences (LIPI), Kawasan Puspiptek Gedung 440-442 Serpong Tangerang Selatan Banten 15314, Indonesia.

^{2,3}Department of Physics, Faculty of Mathematics and Natural Science, Universitas Sumatera Utara 20155, Indonesia

Abstract. The synthesis of soft magnetic $\text{Ni}_x\text{Zn}_{1-x}\text{Fe}_2\text{O}_4$ with variations in composition ($x = 0,2 - 0,8$) by the co-precipitation method has been carried out. The research objective was to determine the effect of x variation on the crystal structure, microstructure, magnetic properties, and density. The samples were characterized by their crystal structure using XRD, microstructure using FE-SEM, magnetic properties using VSM, and physical properties (True Density). The XRD analysis results obtained two phases, the major phase is nickel-zinc ferrite, and Fe_2O_3 shows as the minor phase. The crystal size increased and the lattice parameters decreased with the increase in nickel content. The results of FE-SEM analysis at $x = 0.2$ are spherical in shape with an average particle size found about 47.07 nm. The results of VSM analysis showed that the increase in nickel content, the higher the magnetization saturation value, and the super-paramagnetic properties of all samples obtained. The results of the analysis of physical properties show that true density decreases with an increase of nickel content in each sample.

Keyword: Nanoparticles, Soft-magnetic, Nickel Zinc Ferrite, Co-precipitation, Super-paramagnetic.

Received 5 February 2021 | Revised [19 February 2021] | Accepted [25 February 2021]

1 Introduction

Ferrite spinel nanoparticles have the structural formula MFe_2O_4 (M is a divalent metal ion, including Ni, Co, Cu, Mg, Zn, Mn, Fe) with a cubic spinel crystal structure. Ferrite spinel nanoparticles have superior properties such as high electrical resistivity, high permeability and negligible loss of eddy current. The propagation of high frequency electromagnetic waves makes this material very potential for application in data storage technology, microwave equipment, telecommunications equipment, drug delivery systems, ferro-fluid technology, and gas sensors. Nanoparticles have the potential to be applied in the clinical field if they have a narrow size distribution and super-paramagnetic properties. Iron sand is sand with a high iron

*Corresponding author at: Kawasan Puspiptek Gedung 440-442 Serpong Tangerang Selatan Banten 15314, Indonesia.

E-mail address: nining.s.asri@gmail.com

content. Usually the color is dark gray or blackish in color. This sand consists of Fe_3O_4 magnetite and also contains small amounts of titanium, silica, manganese, calcium, and vanadium [1-4].

$\text{NiZnFe}_2\text{O}_4$ nanoparticles are soft magnetic materials with low coercivity and saturation magnetization but have high electrical resistivity, making this material very suitable for applications in magnetic and magneto-optics fields. Many methods have been developed to synthesize $\text{NiZnFe}_2\text{O}_4$ nanoparticles such as the combustion method, the co-precipitation method, the sol-gel auto-combustion method and the hydrothermal method [5].

Co-precipitation is one of the methods used to make nanoparticle material preparations. The working principle of this method is to convert a metal salt into a precipitate using a hydroxide or carbonate base precipitate which is then converted to its oxidized form by heating. The co-precipitation method is the most effective method because this method can be used in normal environmental conditions.

Synthesis of magnetite nanoparticles using the co-precipitation method is expected to have mono dispersive properties. Mono dispersive properties mean that the magnetite particles are evenly or uniformly distributed. The resulting precipitate is influenced by the concentration of solvent and precipitant, heating temperature, and the duration of stirring. The co-precipitation method with various concentrations of iron salt solutions and settling solutions affects the amount of powder and the magnetic properties of the magnetite formed [6-10].

Materials can have natural or artificial magnetic properties (electromagnets). Magnets are also an advanced material that is very important for a variety of advanced technological applications, functioning as a component in converting motion energy into electricity and vice versa, such as: automotive, electronics and energy [11-13].

In this research, we synthesis ferrite composite of $\text{Ni}_x\text{Zn}_{1-x}\text{Fe}_2\text{O}_4$ with variation of composition ($x = 0.2 - 0.8$) from natural iron sand using simple co-precipitation method. The aim of the parameter is to investigate the effect of the substitution value of x on the structure and magnetic properties of nickel-zinc ferrite.

2 Methods

The materials used in this study were Lombok Krاندangan Iron Sand, $\text{NiCl}_2 \cdot 6\text{H}_2\text{O}$ (Nickel Chloride Hexahydrate), ZnCl_2 (Zinc Chloride), HCl (Hydrochloric Acid), NaOH (Sodium Hydroxide), and aquades. Dissolved 8 grams of iron sand that has been crushed until smooth with 25 ml of 37% HCl . Then the mixture is stirred with a stirring rod until it is homogeneous for about 20 minutes.

Table 1. Sample Mass Calculation $\text{Ni}_x \text{Zn}_{1-x} \text{Fe}_2\text{O}_4$

Sample $\text{Ni}_x \text{Zn}_{1-x} \text{Fe}_2\text{O}_4$	$\text{NiCl}_2 \cdot 6\text{H}_2\text{O}$ (g)	ZnCl_2 (g)
x = 0.2	1.615	3.707
x = 0.4	3.230	2.780
x = 0.6	4.846	1.854
x = 0.8	6.461	0.927

Each mass of the two materials is mixed and dissolved with 25 ml of distilled water until homogeneous. The solution is mixed with a solution of iron sand and stirred for about 20 minutes until a brownish-orange solution is formed. This solution is used as a precursor to the synthesis of nickel-zinc ferrite. Further, 30 g NaOH was dissolved in 250 ml distilled water at 80°C and 500 rpm for 20 minutes. Then the co-precipitation method is carried out by dropping the nickel-zinc ferrite salt solution, drop by drop for about 20-30 minutes into the NaOH solution (in a stirring state) to form a black nickel-zinc ferrite precipitate. Then the temperature was increased to 100°C for 1 hour and 40 minutes.

The precipitate was washed several times with distilled water. Then dried in an oven at 80°C for 2 days until dry. Further, the dried sample is crushed to form a powder. Samples that have been dried and cooled at room temperature are characterized for their physical properties (density), crystal structure (X-Ray Diffraction), microstructure (FE-SEM), and magnetic properties (VSM - Vibrating Sample Magnetometer).

3 Result and Discussion

3.1. True Density

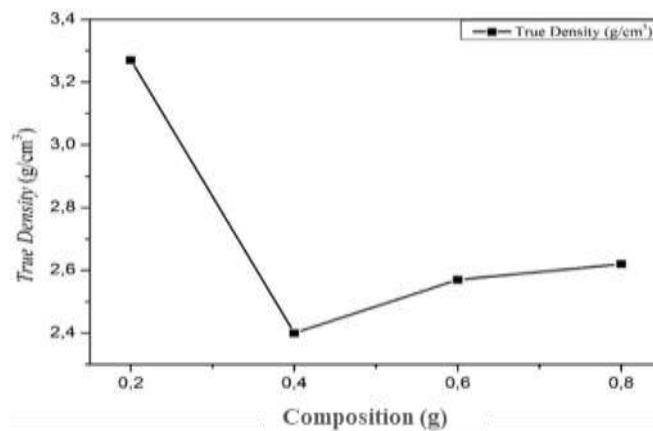


Figure 1. Measurement results of true density against composition x

Figure 1 shows a decrease in density with variations in composition. The density decreased along with the decrease in zinc levels in each sample because the zinc density was greater than the nickel density and the temperature used at the time of measurement was 21°C. Based on the

data sheet from Sigma-Aldrich with code number 641669-10G the density of Nickel Zinc Ferrite at 25°C is 2.81 g/cm³ and we can see in Figure 1 that the density value of each composition is close to the value of the data sheet.

3.2. X- Ray Diffraction (XRD)

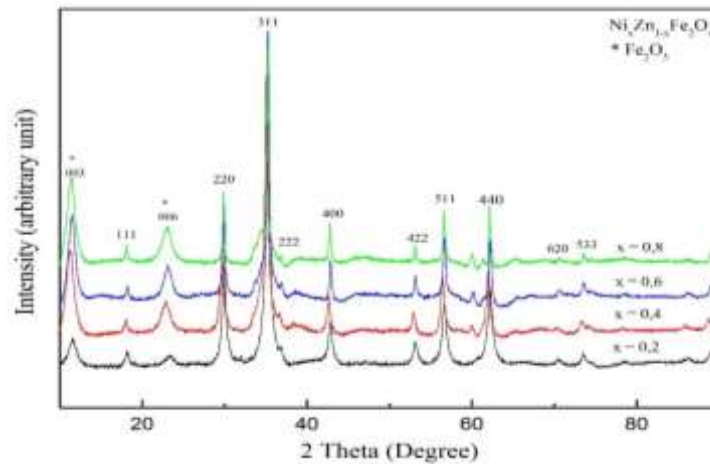


Figure 2. XRD pattern of nikel zinc ferrite ($\text{Ni}_x\text{Zn}_{1-x}\text{Fe}_2\text{O}_4$)

Figure 2 is the result of XRD characterization. The graph obtained is in accordance with the JCPDS reference (PDF Card No. 00-008-0234 Quality: I) and the main peak miller index value in area 2θ is the peak of the plane (311) of each sample. Based on the PDF, the other peaks identified in the pure nickel zinc ferrite ($\text{Ni}_x\text{Zn}_{1-x}\text{Fe}_2\text{O}_4$) nanoparticle samples were fields (111), (220), (222), (400), (422), (511), (440), (613) and (533).

The difference in intensity occurs because the mass of nickel is increasing. By increasing the mass of nickel will increase the crystal size resulting in increased intensity. The increase in intensity also has an effect on the increase in the magnetization saturation value as evidenced by the results of VSM characterization.

Figure 2 shows the appearance of another diffraction pattern at (003) and (006) for each variation, the new peak indicated as Fe₂O₃ (Hematite) peaks according to the reference (PDF Card No. 04-013-3305 Quality: I). This happens because in the process of washing the sediment there is air entering so that oxidation occurs in the sample. As quoted that distilled water and acetone are needed followed by heating at room temperature in the process of washing the precipitates so that the residue can be lost [14,15].

Based on the analysis of XRD data, the soft magnetic nanoparticle sample $\text{Ni}_x\text{Zn}_{1-x}\text{Fe}_2\text{O}_4$ has a cubic crystal structure. Calculation of lattice parameters on the soft magnetic of $\text{Ni}_x\text{Zn}_{1-x}\text{Fe}_2\text{O}_4$ nanoparticle sample using the Cohen method. The determination of crystal size can be determined using the Scherrer equation. Based on the Scherrer equation, the crystallite size is shown in Figure 3, the increasing crystal size is obtained. This shows that the crystal grain size

of $Ni_xZn_{1-x}Fe_2O_4$ increases with increasing nickel content and decreases when zinc levels increase [15].

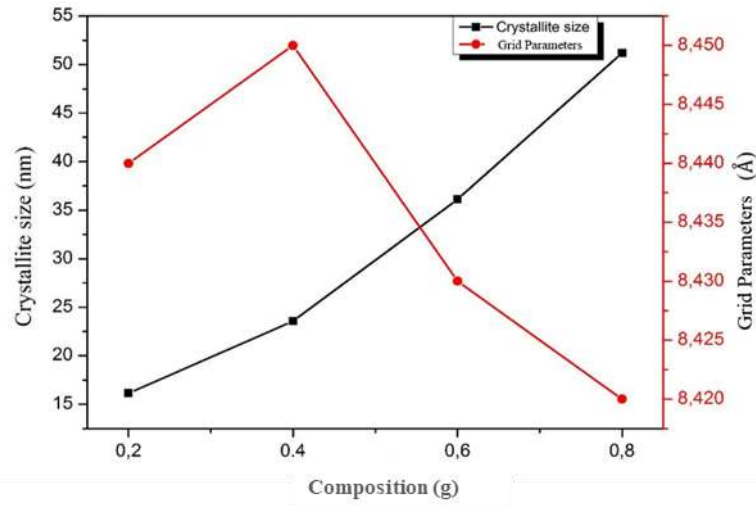


Figure 3. Graph of crystal size calculation and lattice parameters on sampel $Ni_xZn_{1-x}Fe_2O_4$

3.3. Field Emission Scanning Electron Microscope (FESEM)

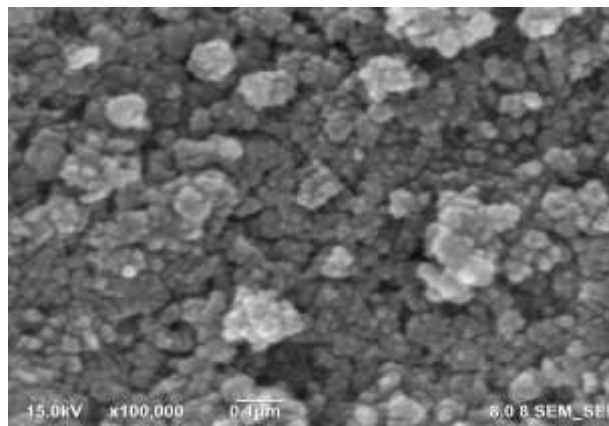


Figure 4. FE-SEM image of $Ni_xZn_{1-x}Fe_2O_4$ ($x = 0.2$)

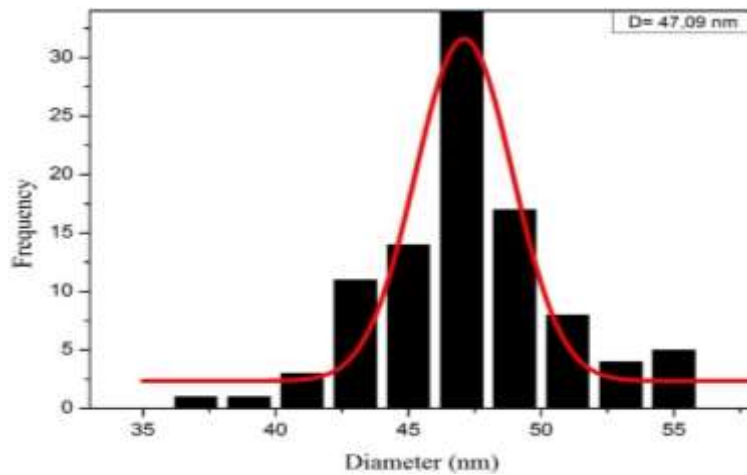


Figure 5. The histogram of grain size of $Ni_xZn_{1-x}Fe_2O_4$ ($x = 0,2$)

The surface morphology of sample $x = 0.2$ was observed by FE-SEM as shown in Figure 4. The particles formed a nearly spherical average shape. The average particle size was analyzed by

ImageJ, and the histogram is shown in Figure 5. The average size of the particle size by histogram analysis is found about 47.09 nm. The result has good agreement with Deshmukh (2017) which found the average particle size for nickel-zinc ferrite is between 41-74.6 nm. From the results, it can be seen that particle size contains multi crystals, which compared to the XRD results for a crystal size $x = 0.2$ of 16.14 nm [15].

3.4. Vibrating Sample Magnetometer (VSM)

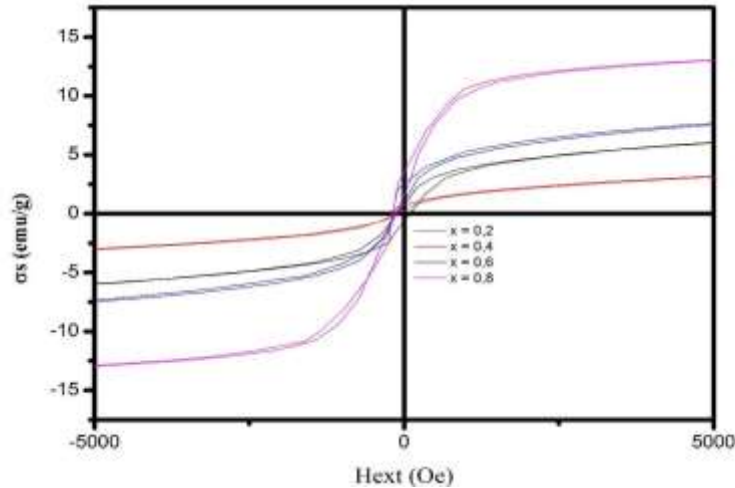


Figure 6. Hysteresis Curve of $\text{Ni}_x \text{Zn}_{1-x} \text{Fe}_2\text{O}_4$ ($x = 0.2 - 0.8$)

Figure 6 shows that the saturation magnetization value from $x = 0.4 - 0.8$ is getting bigger as the nickel content increases in the sample so that the magnetic properties are getting stronger. At $x = 0.2$ the graph is greater than $x = 0.4$ because the impurity phase is lower than $x = 0.4$. The coercivity value of each sample is very small which is a characteristic of soft magnetic and tends to fluctuate. The coercivity value is not linear in the sample, this is estimated because of the impurity phase Fe_2O_3 in each sample. This phase has antiferromagnetic properties because the properties of the impurities are different from the nickel zinc ferrite properties, so it will contribute to each sample. In this study, a soft magnetic field with magnetic properties is superparamagnetic with an increased saturation value, small coercivity and remanence and a value close to previous studies [16-20].

4 Conclusion

The nanoparticle of $\text{Ni}_x \text{Zn}_{1-x} \text{Fe}_2\text{O}_4$ ($x = 0.2 - 0.8$) has been successfully synthesis. The density measurement obtained the density value decrease by the increase of nickel content. The XRD results show the nickel-zinc ferrite phase, however, there another impurity peak is known as Fe_2O_3 (hematite). The crystal size of the sample from $x = 0.2 - 0.8$ was increased and the lattice parameters decreased with the increasing nickel content. The FE-SEM results showed that the average particle size of the sample with the variation of $x = 0.2$ about 47.09 nm, and formed a nearly spherical shape in form. The magnetic properties from the VSM characterization resulted that the magnetization saturation increased along with the increase of nickel content. In

addition, the magnetic properties of nickel-zinc ferrite show super-paramagnetic behavior with narrow coercivity in shape.

REFERENCES

- [1] J. Wan, X. Jiang, H. Li, and K. Chen, "Facile synthesis of zinc ferrite nanoparticles as non-lanthanide T1 MRI contrast agents", *Journal of Material Chemistry*, vol. 22, pp.13500-13505, 2012.
- [2] S.S. Muflihatun and E. Suharyadi, "Sintesis Nanopartikel Nickel Ferrite (NiFe₂O₄) dengan Metode Kopresipitasi dan Karakterisasi Sifat Kemagnetannya", *Jurnal Fisika Indonesia*, vol. 19, no.55, pp.20-25, 2015.
- [3] F. Rozi and A. Budiman, "Pengaruh Variasi Temperatur Terhadap Bentuk Bulir Mineral Magnetik Pasir Besi" *Jurnal Fisika Unand*, vol. 4, no. 2, 2015.
- [4] J. Jumaida, W. Wahyu, and E. Mukhtar, "Pengaruh Suhu Sintering terhadap Struktur dan Sifat Magnetik Material Mn-Zn Ferit", *Prosiding Pertemuan Ilmiah XXVIII HFI Jateng & DIY, Yogyakarta*, vol. 26, 2014.
- [5] N. Tarigan. Efek Komposisi terhadap Sifat Fisis dan Mikrostruktur Serbuk Nanokomposit BaFe₁₂O₁₉/Ni_{0.5}Zn_{0.5}Fe₂O₄, Skripsi, Universitas Sumatera Utara, Program Sarjana, 2018.
- [6] S.K.W. Ningsih, Sintesis Anorganik, Padang: UNP Press, 2016.
- [7] A. Mairoza and A. Astuti, "Sintesis Nanopartikel Fe₃O₄ dari Batuan Besi Menggunakan Asam Laurat sebagai Zat Aditif", *Jurnal Fisika Unand*, vol. 5, no.3, pp.283-286, 2016.
- [8] S. Merdekani and F.J.K.U. Jatinangor, "Sintesis Partikel Nanokomposit Fe₃O₄/SiO₂ dengan Metode Kopresipitasi", *Pros. Semin. Nas. Sains Dan Teknol. Nukl. PTNBRBATAN*, 2013.
- [9] M. P. Aji, Kajian Sifat Magnetik Magnetit (Fe₃O₄) Hasil Penumbuhan Dengan Metode Presipitasi Berbahan Dasar Pasir Besi, Thesis, Institut Teknologi Bandung, 2008.
- [10] Suharyana, Dasar-Dasar Dan Pemanfaatan Metode Difraksi Sinar-X, Surakarta: Universitas Sebelas Maret, 2012.
- [11] E. Afza, Pembuatan Magnet Permanent Ba-Hexafarite (Ba_{0.6}Fe₂O₃) Dengan Metode Kopresipitasi Dan Karakterisasinya, Skripsi, Medan, Universitas Sumatera Utara, 2011.
- [12] H. V. V. Lawrence, Elemen-elemen Ilmu dan Rekayasa Material, Edisi Keenam, Erlangga, Jakarta, 2004.
- [13] S. J. Collocott, J. B. Dunlop, H. C. Lovatt, and V. S. Ramsden, "Rare-earth permanent magnets: new magnet materials and applications", In *Materials Science Forum*, Vol. 315, pp. 77-83, 1999.
- [14] Y. Jamil, M. R. Ahmad, A. Hafeez, and A. N. Zia-ul-Haq, "Microwave assisted synthesis of fine magnetic manganese ferrite particles using co-precipitation technique", *Pakistan Journal of Agricultural Sciences*, vol. 45, no. 3, pp.59-64, 2008.
- [15] S. S. Deshmukh, A. V. Humbe, A. Kumar, R. G. Dorik, and K. M. Jadhav, "Urea assisted synthesis of Ni_{1-x}Zn_xFe₂O₄ (0 ≤ x ≤ 0.8): Magnetic and Mössbauer investigations", *Journal of Alloys and Compounds*, vol. 704, pp.227-236, 2017.
- [16] T. Dippong, E. A. Levei, I. G. Deac, F. Goga, and O. Cadar, "Investigation of structural and magnetic properties of Ni_xZn_{1-x}Fe₂O₄/SiO₂ (0 ≤ x ≤ 1) spinel-based nanocomposites", *Journal of Analytical and Applied Pyrolysis*, vol. 144, pp.104713, 2019.
- [17] B. M. Slusarek, P. Gawrys, and M. Przybylski, "The investigation of Nd-Fe-B dielectromagnets in negative temperature", *Advances In Powder Metallurgy And Particulate Materials*, vol. 2, pp.10, 2007.
- [18] H. Syukriani, A. Budiman, and D. Puryanti, "Pengaruh Temperatur Sintering Terhadap Suseptibilitas Magnetik dan Struktur Stronsium Ferit (SrFe₁₂O₁₉) Pasir Besi Batang Sukam Kabupaten Sijunjung Sumatera Barat", *Jurnal Fisika Unand*, vol. 6, no. 3, pp.225-231, 2017.
- [19] A. L. Bement, Magnetic Materials. Washington D.C. National: Academic Press, 1985.
- [20] A. Bajorek, C. Berger, M. Dulski, P. Łopadczak, M. Zubko, K. Prusik, M. Wojtyniak A.

Chrobak, F. Grasset, and N. Randrianantoandro, "Microstructural and magnetic characterization of Ni_{0.5}Zn_{0.5}Fe₂O₄ ferrite nanoparticles", *Journal of Physics and Chemistry of Solids*, vol. 129, pp.1-21, 2019.